Inorg. Chem. **2003**, *42*, 283–293

"Stapled" Bis(phthalocyaninato)niobium(IV), Pc_2Nb: X-ray Crystal Structure, Chemical and Electrochemical Behavior, and Theoretical Studies. Perspectives for the Use of Pc_2Nb (Thin Films) as an "Optically Passive Electrode" in Electrochromic Devices

Elvira M. Bauer,[†] Maria Pia Donzello,[†] Claudio Ercolani,*[,†] Enrico Masetti,[‡] Stefania Panero,*[,†] Giampaolo Ricciardi,[§] Angela Rosa,*[,§] Angiola Chiesi-Villa,[||] and Corrado Rizzoli[||]

Dipartimento di Chimica, Università degli Studi di Roma "La Sapienza", p.le A. Moro 5, I-00185 Roma, Italy, Laboratorio Dispositivi Ottici, ENEA, via Anguillarese 301, I-00060 Roma, Italy, Dipartimento di Chimica, Università della Basilicata, Via N. Sauro 85, I-85100 Potenza, Italy, and Dipartimento di Chimica Generale ed Inorganica, Università di Parma, Viale delle Scienze, I-43100 Parma, Italy

Received February 1, 2002

Recrystallization of the previously reported monosolvated bis(phthalocyaninato)niobium(IV), $[Pc_2Nb]\cdot ClNP$ (ClNP = 1-chloronaphthalene), has allowed isolation of a single crystal of a new solvated form, i.e. $[Pc_2Nb]\cdot 3.5ClNP$, whose structure has been elucidated by X-ray work: space group $P2_1/n$ (No. 14); $a = 16.765(3)$, $b = 23.800(4)$, $c = 19.421(4)$ Å; $\alpha = \gamma = 90°$, $\beta = 92.51(2)°$; $Z = 4$. The sandwiched material is a "stapled" molecule, characterized by the presence of two intramolecular interligand C–C σ bonds and highly strained phthalocyanine units, as formerly observed by crystallographic work for its Ti(IV) analogue, $[Pc_2Ti]$, and the +1 corresponding fragment, $[Pc_2Nb]^+$, present in the species $[Pc_2Nb](I_3)(I_2)_{0.5}\cdot 3.5ClNP$. $[Pc_2Nb]$ appears to be reluctant to undergo further oxidation above the +1 oxidation state. Detailed theoretical studies by DFT and TDDFT methods have been developed on $[Pc_2Nb]$ and $[Pc_2Nb]^+$, also extended for comparison to the Ti(IV) complex $[Pc_2Ti]$, and an adequate picture of the ground-state electronic structure of these species has been achieved. Moreover, the excitation energies and oscillator strengths calculated for the closed-shell systems, $[Pc_2Ti]$ and $[Pc_2Nb]^+$, provide a satisfactory interpretation of their characteristic visible optical spectra and help to rationalize the similar features observed in the visible spectrum of the open-shell "stapled" complex, $[Pc_2Nb]$. Thin solid films (100–250 nm) of $[Pc_2Nb]$ deposited on ITO (indium-doped tin oxide) show a reversible redox process in neutral or acidic aqueous electrolytes. The electrochemical and electrochromic properties of the sandwiched complex, combined with impedance and UV/visible spectral measurements, are presented and discussed. The achieved electrochemical information, while substantially in keeping with the observed chemical redox behavior and theoretical predictions, qualifies $[Pc_2Nb]$ as an "optically passive" electrode and a promising material for its use in electrochromic devices.

Introduction

At the time of its publication,[1] bis(phthalocyaninato)-titanium(IV), $[Pc_2Ti]$, isolated as a monosolvate species, i.e. $[Pc_2Ti]\cdot ClNP$ (ClNP = 1-chloronaphthalene), was, among the ditetrapyrrolic species of formula L_2M, L being a porphyrin or phthalocyanine macrocycle, an unprecedented example of a sandwiched "stapled" molecule (Figure 1) which exhibits (i) two intramolecular interligand C−C σ bonds, (ii) highly distorted macrocyclic units, quite recently approached also in new Ni(II) phthalocyanine species of formula $[14,28\text{-}(RO)_2PcNi]$ (R = MeO, EtO),[2] (iii) an unusual yellow-orange color, and (iv) peculiar UV−visible

* To whom correspondence should be addressed. E-mail: claudio.ercolani@uniroma1.it (C.E.).
[†] Università degli Studi di Roma "La Sapienza".
[‡] ENEA.
[§] Università della Basilicata.
[||] Università di Parma.

(1) Ercolani, C.; Paoletti A. M.; Pennesi, G.; Rossi, G.; Chiesi-Villa, A.; Rizzoli, C. *J. Chem. Soc., Dalton Trans.* **1990**, 1971.
(2) Molek, C. D.; Halfen, J. A.; Loe, J. C.; McGaff, R. *J. Chem. Soc., Chem. Commun.* **2001**, 2644.

10.1021/ic020098d CCC: $25.00
Published on Web 12/20/2002

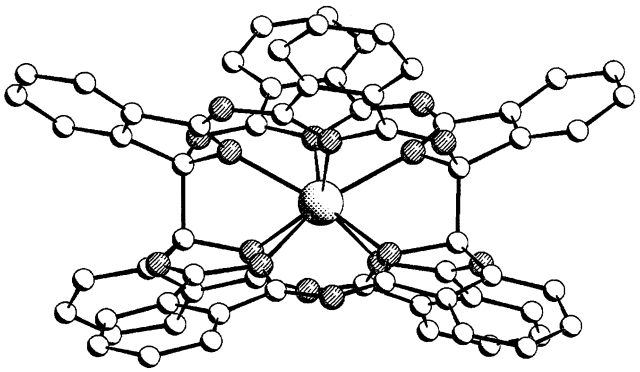

Figure 1. Sketched side view of "stapled" [Pc_2M] molecules (M = Ti, Nb).

spectral features. Additional aspects of interest are (v) quite interesting redox properties (in fact, [Pc_2Ti] undergoes a chemically reversible partial oxidation by reaction with I_2, with formation of an electrically conducting material of formula [Pc_2Ti](I_3)$_{2/3}$, of known structure,[3] characterized by monodimensionally developed chains of [Pc_2Ti]$^{+0.66}$ units, in which considerable elongation of the interligand C−C σ has occurred, and parallel chains of interconnected I_3^- ions) and (vi) remarkable electrochromic behavior.[4]

We recently brought to knowledge the existence of a new "stapled" molecule, i.e. bis(phthalocyaninato)niobium(IV), [Pc_2Nb] (d^1; $\mu_{eff} = 1.69\ \mu_B$), isolated as a crystalline powder of formula [Pc_2Nb]·ClNP,[5] also characterized by unusual color (orange-brown) and UV−visible behavior, but were unable to have a precise knowledge of the molecular details. Substantial incremental support to the assigned peculiar structure was given later by single-crystal X-ray work on the diamagnetic product formed by monoelectronic oxidation of [Pc_2Nb], i.e. [Pc_2Nb](I_3)(I_2)$_{0.5}$·3.5ClNP, in which the [Pc_2Nb]$^+$ cationic fragment also exhibits intramolecular C−C σ bonds in a "stapled" arrangement.[6]

Efforts for the isolation of single crystals of the unoxidized material [Pc_2Nb] suitable for X-ray work were previously announced,[5] and it has been only recently that an ampule closed years earlier revealed the presence of several (8−10) small crystals of the species, only one among them found big enough for X-ray examination. Elucidation of the structure of the species presented here, to be formulated as the solvate [Pc_2Nb]·3.5ClNP, definitely confirms the "stapled" nature of the sandwiched species. Examination of its electrochemical behavior, also detailed here, provides evidence for some peculiar electrochromic properties, to be compared with those of the related Ti(IV) species.[4] One noticeable feature, needed to be more deeply examined, is the observed marked inertness of the monocation [Pc_2Nb]$^+$ to either chemical or electrochemical further oxidation. The need for an adequate interpretation of the electronic structure of the [Pc_2Nb] and [Pc_2Nb]$^+$ units and a satisfactory explanation of the observed unusual UV−visible spectral and redox behavior has led to a detailed theoretical study, based on DFT and TDDFT calculations. As a result, elucidation of the ground-state electronic structure for both species has been accomplished, appropriately accompanied by similar achievements on the Ti(IV) analogue, [Pc_2Ti]. As will be also shown below, the previously suggested metal-centered oxidation for the process [Pc_2Nb] → [Pc_2Nb]$^+$,[6] is further considered. In addition, easy explanation is provided for the inertness of [Pc_2Nb] to form more positively charged species above the +1 cation [Pc_2Nb]$^+$. Last, but not the least, the electrochromic behavior of [Pc_2Nb] identifies this species as a promising material to be used as a "passive electrode" in display devices.

Experimental Section

Pure grade reagents and solvents were used. Phenoxathiin hexachloroantimonate, (Phenox)$SbCl_6$, was obtained as reported elsewhere.[7]

Synthetic Aspects. [Pc_2Nb]·ClNP and [Pc_2Nb]·3.5ClNP. Bis(phthalocyaninato)niobium(IV), prepared in hot ClNP and purified as described in detail elsewhere,[5,6] is obtained as a microcrystalline powder in the form of a monosolvate of formula [Pc_2Nb]·ClNP. For the preparation of single crystals for X-ray work, innumerable attempts of recrystallization were made from the same solvent (ClNP), and as anticipated above, in an ampule closed years before and recently reexamined, just one suitable single crystal was found present, together with a few (8−10) much smaller crystals. Evidently, slow crystallization has allowed incorporation of a different amount of solvent in the crystal, since, once the structure was solved by X-rays, the crystal showed its correct composition to be [Pc_2Nb]·3.5ClNP.

[Pc_2Nb]ClO_4·2DMF. This species was prepared by suspending 30 mg (0.024 mmol) of [Pc_2Nb]·ClNP in 20 mL of dimethyl formamide (DMF), 4 mL of H_2O, and 5−6 drops of $HClO_4$ (70%). The mixture was kept under stirring for 3 h at 50−60 °C. On cooling, the yellow-green solid material was separated by centrifugation, washed with acetone, and brought to constant weight under vacuum (19 mg). Anal. Calcd for the formula [Pc_2Nb]ClO_4·2DMF, $C_{70}H_{46}ClN_{18}NbO_6$: C, 61.67; H, 3.40; N, 18.49. Found: C, 61.80; H, 3.43, N, 19.18.

[Pc_2Nb]BF_4·2DMF. A suspension of [Pc_2Nb]·ClNP (33 mg, 0.026 mmol) in 20 mL of DMF, 4 mL of H_2O, and 2 drops of $HClO_4$ (70%) was kept under stirring for 3 h in the presence of a large excess of [Bu_4N]BF_4 at 50−60 °C. On cooling, the yellow-mustard solid was separated by centrifugation, washed with acetone, and brought to constant weight under vacuum (15 mg). Anal. Calcd for the formula [Pc_2Nb]BF_4·2DMF, $C_{70}H_{46}BF_4N_{18}NbO_2$: C, 62.23; H, 3.43; N, 18.66. Found: C, 61.79, H, 3.34, N, 18.55.

[Pc_2Nb]PF_6. A suspension of [Pc_2Nb]·ClNP (33 mg, 0.026 mmol) in 20 mL of DMF, 4 mL of H_2O, and 2 drops of $HClO_4$ (70%) was kept under stirring for 3 h in the presence of a large excess of NH_4PF_6 at a temperature of 50−60 °C. On cooling, the olive-green solid was separated by centrifugation, washed with acetone, and brought to constant weight under vacuum (13 mg). Anal. Calcd for the formula [Pc_2Nb]PF_6, $C_{64}H_{32}F_6N_{16}NbP$: C, 60.87; H, 2.55; N, 17.74. Found: C, 60.94; H, 2.47; N, 17.72.

(3) Capobianchi, A.; Ercolani, C.; Paoletti, A. M.; Pennesi, G.; Rossi, G.; Chiesi-Villa, A.; Rizzoli, C. *Inorg. Chem.* **1993**, *32*, 4605.
(4) Capobianchi, A.; Paoletti, A. M.; Pennesi, G.; Rossi, G.; Panero, S. *Synth. Met.* **1995**, *75*, 37.
(5) Donzello, M. P.; Ercolani, C.; Lukes P. J. *Inorg. Chim. Acta* **1997**, *256*, 171.
(6) Donzello, M. P.; Ercolani, C.; Chiesi-Villa, A.; Rizzoli C. *Inorg. Chem.* **1998**, *37*, 1347.
(7) Gans, P.; Marchon, J.-C.; Reed, C. A.; Regnard, J.-R. *Nouv. J. Chim.* **1981**, *5*, 203.

Table 1. Crystallographic Data for $[Pc_2Nb]\cdot 3.5ClNP$

formula	$C_{64}H_{32}N_{16}Nb\cdot 3.5C_{10}H_7Cl$
a, Å	16.765(3)
b, Å	23.800(4)
c, Å	19.421(4)
α, *γ*, deg	90
β, deg	92.51(2)
V, Å^3	7742(2)
Z	4
fw	1687.1
space group	$P2_1/n$ (No. 14)
T, °C	22
λ, Å	0.710 69
D_{calc}, g cm^{-3}	1.448
μ, cm^{-1}	3.31
R[a]	0.052
wR_2[b]	0.141

[a] $R = \sum|\Delta F|/\sum|F_o|$. [b] $wR_2 = [\sum w|\Delta F^2|^2/\sum w|F_o^2|^2]^{1/2}$.

$[Pc_2Nb]SbCl_6$. A suspension of $[Pc_2Nb]\cdot ClNP$ (20 mg, 0.0156 mmol) in 10 mL of freshly distilled benzene was kept under stirring for 48 h in the presence of $(Phenox)SbCl_6$ (8.3 mg, 0.0156 mmol) at room temperature. After centrifugation of the suspension, the orange-brown solid material was washed twice with acetone and brought to constant weight under vacuum (8.9 mg). Anal. Calcd for the formula $[Pc_2Nb]SbCl_6$, $C_{64}H_{32}Cl_6N_{16}NbSb$: C, 52.93; H, 2.22; N, 15.43. Found: C, 53.52; H, 2.45; N, 14.96. The same reaction carried out by using the reactants $[Pc_2Nb]\cdot ClNP$ and $(Phenox)SbCl_6$ in a 1:2 molar ratio led to the formation of the same oxidized species $[Pc_2Nb]SbCl_6$ with no trace of the formation of the doubly charged cation $[Pc_2Nb]^{2+}$.

As expected, all the above oxidized species show a substantially identical IR spectrum in all the regions explored (4000−200 cm^{-1}) due to the identical $[Pc_2Nb]^+$ cation present. Distinct additional absorptions are present only due to the solvent molecules (DMF, very strong absorption at 1670 cm^{-1}) and to the different anions (ClO_4^-, very intense absorption with peak maximum at 1100 cm^{-1}; BF_4^-, 1055 cm^{-1} (vs); PF_6^-, 840 cm^{-1} (vs); $SbCl_6^-$, 350 cm^{-1} (m)). For all the species, the UV−visible spectrum in CH_2Cl_2 solution has been found identical to that observed for the complex $[Pc_2Nb](I_3)(I_2)_{0.5}\cdot 3.5ClNP$[6] also containing the $[Pc_2Nb]^+$ cation.

X-ray Data Collection. Data for $[Pc_2Nb]\cdot 3.5ClNP$ were collected on a Philips PW1100 diffractometer at 295 K using Mo Kα radiation. Solution and refinement were carried out using the programs SHELX76[8] and SHELX93.[9] Table 1 summarizes the structural data for $[Pc_2Nb]\cdot 3.5ClNP$.

Theoretical Model and Computational Details. The density functional calculations reported in this paper were performed with the parallelized Amsterdam Density Functional (ADF) suite of programs, release 2000.02.[10−12] The exchange-correlation functionals contain nonlocal corrections to the local density approximation (LDA). For the latter, the parametrization of Vosko, Wilk, and Nusair[13] was used, whereas for the former use was made of the generalized gradient approximation for exchange by Becke[14] and for correlation by Perdew.[15] Excitation energies and oscillator strengths were computed using a time-dependent density functional (TDDFT) approach as implemented in the ADF code[16,17] and thoroughly reviewed.[18−21] In the TDDFT calculations use was made of the adiabatic local density approximation (ALDA) for the exchange-correlation (xc) kernel and the Becke−Perdew generalized gradient approximated potential for the xc potentials which appear in the zeroth-order Kohn−Sham equations. The ionization potentials were computed using the ΔSCF procedure (ΔSCF means that separate self-consistent calculations are performed to optimize the orbitals of the ground state and the appropriate ionic state determinants).

The atoms were described by the standard ADF IV basis set,[22] which is an uncontracted triple-*ξ* STO basis set, with one 3d polarization function for C and N and one 2p for H atoms, and a triple-*ξ* *n*d, $(n + 1)$s basis, with one $(n + 1)$p function for Ti and Nb. The cores (C, N, 1s; Ti, 1s−2p; Nb, 1s−3d) were kept frozen. The calculations have been performed for the C_1 experimental geometry of the molecules.

Electrochemical Studies. (a) Preparation and Spectroscopic Characterization of Thin Films of $[Pc_2Nb]$. $[Pc_2Nb]$ was obtained from $[Pc_2Nb]\cdot ClNP$, by heating the latter at 300 °C for 1 h under vacuum (10^{-5} mbar), and its chemical integrity was checked by elemental analyses and IR/UV−visible spectra. For the preparation of thin films (thickness 50−250 nm), $[Pc_2Nb]$ was deposited by thermal evaporation on ITO (indium-doped tin oxide) covered glass slides (20 Ω/square). Parallel depositions were performed on NaCl (Hellma) and optical glass disks (B270, IRLBAKER), for the check of the IR and UV−visible spectral response, respectively. Glass slides were first washed with a detergent, rinsed with deionized water, and dried. All substrates were cleaned with anhydrous ethanol before deposition. The depositions were performed at 500−550 °C under ca. 10^{-4} mbar, using Ar as an inert transporting medium. The substrates were initially at room temperature and eventually reached mild temperatures (<100 °C) during sublimation. Film thickness was monitored by an INFICON quartz crystal microbalance using a density of 1.7 g/cm^3 and controlled after deposition by a Tencor alpha-step 200 profilemeter.

IR spectra were recorded on a Perkin-Elmer FTIR Spectrum One. For all samples of thin films of $[Pc_2Nb]$, good correspondence of the IR spectra was always observed before and after deposition. Spectral comparison for the $[Pc_2Nb]$ target material (KBr pellet) and the corresponding thin film on NaCl disk was appropriately made by using the diagnostic peaks present in the region explored (Figure 2), particularly the three medium-to-weak peaks in the 1660−1610 cm^{-1} region and a quintuplet in the range 1100−1000 cm^{-1}, characteristic for the present complex $[Pc_2Nb]$[5] and for $[Pc_2Ti]$ as well.[1] These findings confirm the high thermal stability of $[Pc_2Nb]$ during the deposition process.

UV−visible spectra of the sublimed $[Pc_2Nb]$ films were registered with a Perkin-Elmer Lambda 19 spectrophotometer, and those

(8) Sheldrick, G. M. *shelx76. Program for crystal structure determination*; University of Cambridge: Cambridge, England, 1976.
(9) Sheldrick, G. M. *shelxl93. Program for crystal structure refinement*; University of Göttingen: Göttingen, Germany, 1993.
(10) Baerends, E. J.; Ellis, D. E.; Ros, P. *Chem. Phys.* **1973**, *2*, 41.
(11) te Velde, G.; Baerends, E. J. *J. Comput. Phys.* **1992**, *99*, 84.
(12) Fonseca Guerra, C.; Visser, O.; Snijders, J. G.; te Velde, G.; Baerends, E. J. Parallelization of the Amsterdam Density Functional Program. In *Methods and Techniques for Computational Chemistry*; Clementi, E., Corongiu, G., Eds.; STEF: Cagliari, Italy, 1995; pp 305−395.
(13) Vosko, S. H.; Wilk, L.; Nusair, M. *Can. J. Phys.* **1980**, *58*, 1200.
(14) Becke, A. *Phys. Rev. A* **1988**, *38*, 3098.
(15) Perdew, J. P. *Phys. Rev. B* **1986**, *33*, 8822 (Erratum: *Phys. Rev. B* **1986,** *33*, 7406).
(16) van Gisbergen, S. J. A.; Snijders, J. G.; Baerends, E. J. *J. Chem. Phys.* **1995**, *103*, 9347.
(17) van Gisbergen, S. J. A.; Snijders, J. G.; Baerends, E. J. *Comput. Phys. Commun.* **1999**, *118*, 119.
(18) Casida, M. In *Recent Advances in Density Functional Methods*; Chong, D. P., Ed.; World Scientific: Singapore, 1995; Vol 1, p 155.
(19) Gross, E. K. U.; Khon, W. *Adv. Quantum Chem.* **1990**, *21*, 255.
(20) Gross, E. K. U.; Dobson, J. F.; Petersilka, M. In *Density Functional Theory, Springer Series Topics in Current Chemistry*; Nalewajski, R. F., Ed.; Springer: Heidelberg, Germany, 1996.
(21) Gross, E. K. U.; Ullrich, C. A.; Gossmann, U. J. *NATO ASI Series B*; Plenum: New York, 1995; Vol. 337, p 149.
(22) ADF STO basis set database available on line at http://tc.chem.vu.nl/SCM/Doc/atomicdatabase.

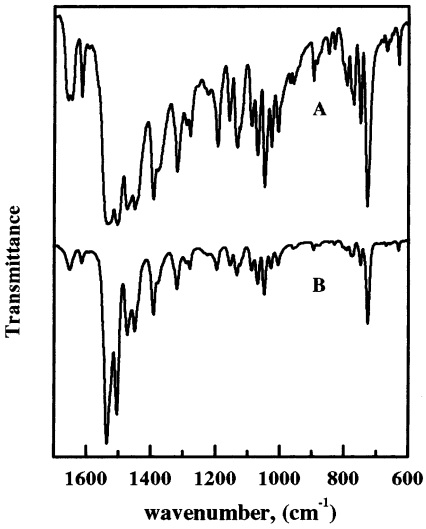

Figure 2. IR spectra of [Pc_2Nb] (KBr pellet, A; film deposited on NaCl disk, B).

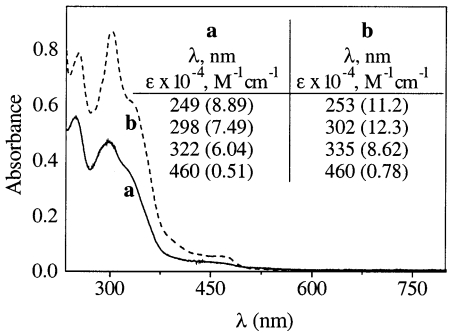

Figure 3. Quantitative UV−visible spectra in CH_2Cl_2 of (a) [Pc_2Nb]·ClNP and (b) [Pc_2Nb](I_3)(I_2)$_{0.5}$·3.5ClNP. Spectral data for [Pc_2Ti]·ClNP are as follows (λ, nm; $10^{-4}\epsilon$, M^{-1} cm^{-1}): 245 (11.3), 294 (9.62), 324 (6.17), 426 (0.69), 467 (0.53).[5]

of solutions in CH_2Cl_2, with a Varian Cary 5 spectrophotometer. The spectra of [Pc_2Nb] films, measured in the region 300−800 nm, show, reproducibly, a very intense and broad absorption with maximum intensity at ca. 320 nm and a weak shoulder, plateau-shaped, in the region 400−500 nm. For rare samples, very weak absorptions were found in the Q-band region (600−700 nm), reasonably attributable to subtle traces of PcH_2, if account is taken of the massive formation of this byproduct during the preparative process and its difficult complete elimination.[6] If dissolved in CH_2Cl_2, the [Pc_2Nb] films show intense absorptions at ca. 250 and 300 nm, a shoulder at ca. 320 nm, and a broad weak plateau in the region 400−500 nm evidencing a little higher intensity at ca. 400 and 460 nm. For a need of comparison, solution spectra in CH_2Cl_2 of unsublimed [Pc_2Nb]·ClNP and of a sample of the complex [Pc_2Nb](I_3)(I_2)$_{0.5}$·3.5ClNP containing the cation [Pc_2Nb]$^+$ are given in Figure 3, with related tabulated quantitative data, incompletely given previously.[5,6] Worthy of notice, examination of qualitative solution spectra in the same solvent of available nice-looking small single crystals of the species [Pc_2Nb]·3.5ClNP and [Pc_2Nb](I_3)-(I_2)$_{0.5}$·3.5ClNP definitely exclude, even under magnification of the spectra, the presence of absorptions for both species in the region 600−800 nm. This confirms that, when observed, weak absorptions in the range 600−700 nm are Q-bands most likely due to traces of an impurity, i.e. PcH_2.

(b) Measurements. The electrochemical experiments were carried out at room temperature in a conventional three-electrode cell; the working electrode was a 1 cm diameter circle ITO glass slide coated with [Pc_2Nb], the reference was a SCE, and a platinum sheet was used as counter electrode. The aqueous electrolytes used in the experiments were prepared by dissolving in doubly distilled water pure grade MCl salts (M = Li, Na, K, tetraethylammonium) (1 M) or acidic media, i.e. HCl (1 M), HNO_3 (0.1 M), and $HClO_4$ (1 M), without further purification. The cyclic voltammetry measurements were carried out using an AMEL 2051 potentiostat coupled with an AMEL 568 function generator. During experiments, the optical characterization of the thin films in the UV−visible region was carried out "in situ" using a Hewlett-Packard 8452 spectrophotometer. The absorbance values quoted in this work refer to the [Pc_2Nb] sample, taking the bare system (cell, ITO electrodes, and electrolyte) as baseline. The impedance spectroscopy was measured by using a Solartron 1255B frequency response analyzer coupled with a Solartron 1286 electrochemical interface over a frequency range extending from 200 mHz to 5 kHz.

Chart 1. ORTEP Side View (50% Probability Ellipsoids) of [Pc_2Nb]

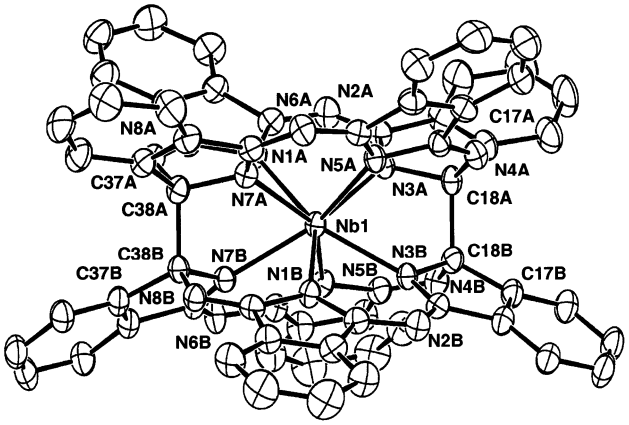

Results and Discussion

Chemical Redox Behavior of [Pc_2Nb]. As shown before,[6] [Pc_2Nb] can be easily chemically oxidized with I_2 in benzene to give the [Pc_2Nb]$^+$ fragment. The present results indicate that a similar monoelectronic oxidation for [Pc_2Nb] is also occurring in DMF by using $HClO_4$ as the oxidant, eventually also in the presence of an excess of $[Bu_4N]BF_4$ or NH_4PF_6, as well as in benzene by reaction with (Phenox)$SbCl_6$, with consequent isolation, respectively, of the saltlike species [Pc_2Nb]ClO_4·2DMF, [Pc_2Nb]BF_4·2DMF, [Pc_2Nb]PF_6, and [Pc_2Nb]$SbCl_6$. In no case was evidence found for the formation of further oxidized species, a fact which must be taken as strongly indicative of the reluctance for [Pc_2Nb] to undergo oxidation above the +1 charged state. There seems to be adequate support for this behavior by theoretical studies and further evidence from electrochemical data (see below).

Molecular Structure of [Pc_2Nb]·3.5ClNP. Chart 1 illustrates the molecular structure of the complex (solvent molecules neglected). Selected bond distances and angles are quoted in Table 2.

Essential information from X-ray data on [Pc_2Nb]·3.5ClNP can be summarized as follows:

(i) The structure consists of [Pc_2Nb] neutral complex molecules (Chart 1) and ClNP solvent molecules of crystallization in the stoichiometric complex/solvent molar ratio of 1/3.5.

Table 2. Selected Bond Distances (Å) and Angles (deg) for $[Pc_2Nb]\cdot 3.5ClNP$

	molecule			molecule	
	A	B		A	B
Nb(1)−N(1)	2.293(2)	2.291(3)	N(4)−C(18)	1.431(5)	1.430(5)
Nb(1)−N(3)	2.221(3)	2.203(2)	N(4)−C(21)	1.285(5)	1.281(5)
Nb(1)−N(5)	2.302(2)	2.285(3)	N(5)−C(21)	1.414(5)	1.421(5)
Nb(1)−N(7)	2.215(3)	2.218(3)	N(5)−C(28)	1.362(4)	1.359(4)
N(1)−C(1)	1.427(5)	1.432(5)	N(6)−C(28)	1.316(5)	1.311(5)
N(1)−C(8)	1.359(5)	1.351(4)	N(6)−C(31)	1.342(5)	1.346(5)
N(2)−C(8)	1.320(5)	1.325(5)	N(7)−C(31)	1.319(4)	1.312(4)
N(2)−C(11)	1.353(5)	1.357(5)	N(7)−C(38)	1.492(5)	1.495(5)
N(3)−C(11)	1.316(4)	1.307(4)	N(8)−C(1)	1.288(5)	1.274(5)
N(3)−C(18)	1.497(5)	1.503(4)	N(8)−C(38)	1.432(4)	1.432(4)
C(18)A−C(18)B	1.578(3)		C(38)A−C(38)B	1.577(3)	

	molecule			molecule	
	A	B		A	B
N(1)−Nb(1)−N(3)	74.5(1)	74.3(1)	N(3)−C(18)−C(17)	103.8(3)	103.9(3)
N(1)−Nb(1)−N(7)	73.5(1)	74.0(1)	N(3)−C(18)−N(4)	115.6(3)	117.5(3)
N(3)−Nb(1)−N(5)	72.9(1)	74.4(1)	N(4)−C(18)−C(17)	109.3(3)	109.3(3)
N(5)−Nb(1)−N(7)	74.8(1)	74.1(1)	N(7)−C(38)−C(37)	104.0(3)	103.9(3)
N(1)−Nb(1)−N(5)	109.7(1)	111.5(1)	N(7)−C(38)−N(8)	115.9(3)	117.3(3)
N(3)−Nb(1)−N(7)	122.5(1)	122.2(1)	N(8)−C(38)−C(37)	109.9(3)	108.8(3)
N(4)A−C(18)A−C(18)B	111.4(3)		N(3)B−C(18) B−C(18)A	100.8(2)	
N(3)A−C(18)A−C(18)B	101.6(3)		N(4)B−C(18) B−C(18)A	108.6(2)	
C(17)A−C(18)A−C(18)B	115.0(3)		C(17)B−C(18)B−C(18)A	116.8(3)	
N(8)A−C(38)A−C(38)B	111.1(3)		N(7)B−C(38) B−C(38)A	101.6(2)	
N(7)A−C(38)A−C(38)B	101.6(3)		N(8)B−C(38) B−C(38)A	109.3(2)	
C(37)A−C(38)A−C(38)B	114.2(3)		C(37)B−C(38)B−C(38)A	116.0(3)	

Table 3. Structural Features of Nb and Ti Bis(phthalocyaninato) Species

compd	av M−N, Å	interligand C−C σ bonds, Å	dist between N_4 planes, Å	rel rotation, deg	refs
$[Pc_2Nb]$	2.254	1.578(3), 1577(3)	2.390	45	tp[a]
$[Pc_2Nb]^+$	2.22	1.574(15)	2.387	45	6
$[Pc_2Ti]$	2.22	1.556(6), 1.575(6)	2.32	45	1
$[Pc_2Ti]^{+0.66}$	2.246	2.839(19)	2.42	41.1	3

[a] tp = this paper.

(ii) The coordination polyhedron provided to the metal by the nitrogen atoms from the N_4 cores of the two phthalocyanine units (hereafter labeled units A and B) approximates a distorted square antiprism (see further discussion below).

(iii) The distance between the least-squares mean planes through the parallel N_4 cores (dihedral angle 0.3(1)°) is 2.390(11) Å, very close to that found for the $[Pc_2Nb]^+$ cation (2.387 Å)[6] and markedly longer, as expected, than that observed for $[Pc_2Ti]$ (2.32 Å) (Table 3).[1] Both cores show a significant distortion from planarity toward a tetrahedral arrangement ranging from −0.129(2) to 0.128(2) Å in A and from −0.110(2) to 0.110(2) Å in B. The metal is displaced by 1.195(1) and 1.178(1) Å from the cores of A and B, respectively.

(iv) The two interunit C−C σ-bonds, occurring at the C(18) and C(38) atoms (C(18)A−C(18)B 1.578(3) Å; C(38)A−C(38)B 1.577(3) Å), "tie" together the Pc units which are arranged in a staggered orientation, as indicated by the angles of 46.6(1) and 45.7(1)° between the N(1)A, N(5)A−N(1)B, N(5)B and N(3)A, N(7)A−N(3)B, N(7)B vectors, respectively.

(v) The presence of two sp^3 carbon atoms within the Pc units completely removes the planarity of the macrocyclic units, as indicated in each one by the outward bending of the isoindole units with respect to the related N_4 core and by the twisting of the phenyl rings. This removal highly affects the chromophoricity of the Pc macrocycle with the already evidenced peculiar UV/visible spectral behavior (absence of Q-bands in the 600−700 nm region).[5]

(vi) The Nb−N bond distances are significantly different. In fact, those involving the opposite N(3) and N(7) nitrogen atoms (mean value 2.212(13) Å) are shorter than those involving the opposite N(1) and N(5) atoms (mean value 2.295(12) Å). This asymmetry was also observed in $[Pc_2Nb]^+$,[6] with shorter corresponding single bond distances and mean values (Nb−N(3) 2.190(7) Å, Nb−N(7) 2.186(8) Å, mean value 2.188 Å; Nb−N(1) 2.232(7) Å, Nb−N(5) 2.280(7) Å, mean value 2.256 Å).

(vii) The trend of the N−C and C−C bond distances within the N(1), C(1), N(8), C(38), N(7) and N(3), C(18), N(4), C(21), N(5) chelation rings is consistent with a double-bond character of the N(8)−C(1) (mean value 1.281(7) Å) and N(4)−C(21) (mean value 1.283(3) Å) bonds, while within the N(1), C(8), N(2), C(11), N(3) and N(5), C(28), N(6), C(31), N(7) chelation rings a substantial delocalization of the π bonds is observed (Table 2).

(viii) The structural features of $[Pc_2Nb]$ closely recall those found for its Ti(IV) analogue[1] and the cation $[Pc_2Nb]^+$,[6] but differ significantly from those of the $[Pc_2Ti]^{+0.66}$ unit.[3] The X-ray data shown in Table 3 indicate that the "integral" monoelectronic oxidation $[Pc_2Nb] \rightarrow [Pc_2Nb]^+$ causes only subtle structural changes (columns II−IV), consisting of a slight shortening of the Nb−N and interligand C−C bond distances and the N_4–N_4 separation, leaving the molecular structure practically unmodified. In comparison, the observed effect of the "partial" oxidation on the Ti(IV) sandwich

[Pc_2Ti] is instead severe, since it determines the breaking of the interligand C−C σ bonds, and the internal form of rearrangement in the solid is markedly modified.[3] Curiously, however, thin solid films of [Pc_2Ti] undergo exclusively "integral" electrochemical processes.[4]

Theoretical Studies on [Pc_2Nb], [Pc_2Nb]$^+$, and [Pc_2Ti]. DFT and TDDFT calculations have faced problems concerning (a) the electronic structure of the present Nb and Ti species and their optical properties, (b) the nature of the oxidation process [Pc_2Nb] → [Pc_2Nb]$^+$, and (c) the observed chemical and electrochemical (see below) reluctance of the [Pc_2Nb]$^+$ cation to undergo further oxidation.

Before discussion of the electronic structure of the "stapled" niobium and titanium bis(phthalocyaninato) complexes, it should be kept in mind that although these species exhibit the typical features of tetrapyrrole sandwich complexes, i.e. the relative twisting and the doming of the two phthalocyanine rings, the presence of the two interligand C−C σ bonds has the important electronic effect of breaking down the delocalization of the π ring system. The consequence is that the character and energy of the frontier orbitals of the interacting phthalocyanine residues differ substantially from those of the "normal" Pc ring of mono(phthalocyanines)[23,24] and of the "unstapled" bis(phthalocyaninato) complexes.[25] In addition, the observed deviation from planarity toward a tetrahedral arrangement of each N_4 core, due again to the interligand C−C σ bonds, causes the coordination environment around the metal ion to sensibly deviate from the square antiprism form, reminiscent of the D_{4d} symmetry, usually observed in "normal" ditetrapyrrolic analogues.[26] In the "stapled" species the metal−N(pyrrolic) bond distances are remarkably different, as already evidenced above, those involving the opposite N atoms of the pyrrolic rings engaged in the interligand C−C σ bonds, hereafter denoted as N_p', being significantly shorter than those involving the N atoms of the other two pyrrolic rings (N_p''), with relevant effects on the features of the metal−ligand interactions and, hence, on the pattern of the frontier MOs.

According to Chart 2, where the top view of the MN_8 subunit of the complex is depicted, while the d_{z^2}, the d_{xy}, and the $d_{x^2-y^2}$ orbitals are suitable for interaction with both the closer nitrogens, N_p', and the further nitrogens, N_p'', the d_{yz} and d_{xz} interact preferentially with either of the two different sets of nitrogens, i.e. the former with the N_p' set and the latter with the N_p'' set. As a result, the d_{yz} is destabilized to a lesser extent by interaction with the pyrrolic nitrogens than the other metal d orbitals, including the d_{z^2}, which in the "unstapled" bis(tetrapyrrole) complexes is the least affected by the eight pyrrolic N donors.[27] The larger involvement of the d_{z^2} in the bonding to the macrocycles as

Chart 2. Top View of the MN_8 Subunit in the Sandwiched Nb and Ti Species

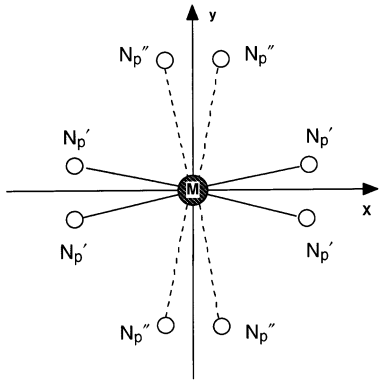

occurs in the "stapled" complexes is due to the exceptionally large doming of the interacting macrocycles which causes the N_p lone pairs to point toward the ring of the d_{z^2} orbital.

The highest occupied and the lowest unoccupied one-electron levels of [Pc_2Nb], [Pc_2Nb]$^+$, and [Pc_2Ti] are shown in Figure 4. For the open-shell system, [Pc_2Nb], spin-unrestricted calculations have been performed, but in Figure 4a the spin-restricted orbital energies are reported for the sake of graphical simplicity. According to the occupation of the one-electron levels, [Pc_2Nb] has a ^2A ground state, the unpaired electron residing in an orbital, the 191a, which is mostly (58%) a metal 4d orbital, with some antibonding admixture of 2p orbitals of the opposite nitrogens of the pyrrolic rings engaged in the interligand C−C σ bonds, the N_p'' set. The metallic character of the 191a comes essentially from the $4d_{yz}$ (34%) and the $4d_{z^2}$ (14%) orbitals, the contribution of the remaining 4d orbitals, which also mix into it owing to the absence of symmetry in the molecule, being much lower. Due to the large Nb-$4d_{yz}$ character, the antibonding with the pyrrolic nitrogens is not so effective and this orbital results as the lowest of the Nb-4d states, which are found in the virtual spectrum at very high energy and therefore are not reported in Figure 4a. As stressed above, the $4d_{z^2}$, $4d_{xy}$, $4d_{x^2-y^2}$, and $4d_{xz}$ orbitals set up stronger interactions with the pyrrolic nitrogens than does the $4d_{yz}$, and hence, they are pushed up considerably. The calculated d-electron configuration of Nb, giving an electron count of one for the doublet ground state, indicates that the Nb atom in [Pc_2Nb] can be formally described as a Nb(IV) (d^1). The self-consistent configuration of $Nb^{2.71+}$ $d^{2.29}$ $s^{0.00}$ $p^{0.00}$ is notably different from the nominal ionic state Nb^{4+} d^1 s^0 p^0. This is because of the covalent bonding interaction between the metal center and the macrocycle, resulting in a Pc_2 → Nb donation of 1.29e. According to the calculated spin density, [Pc_2Nb] has a net spin of 1, localized mostly on Nb (0.85 electrons). This is in accord with magnetic measurements[5] and EPR spectra,[6] both sets of data suggesting the presence of an unpaired electron on the metal center.[6]

As inferred from the level scheme of Figure 4a, in [Pc_2Nb] a very large energy gap (∼1.9 eV) separates the HOMO from the set of the lower six occupied MOs which are a mixture of bridging (*meso)* and pyrrolic N 2p orbitals. As expected, the σ bonding combinations of the "stapling" C_α lie at much lower energy and are not shown in the diagram of Figure

(23) Ricciardi, G.; Rosa, A.; Baerends, E. J. *J. Phys. Chem. A* **2001**, *105*, 3340.
(24) Rosa, A.; Ricciardi, G.; Baerends, E. J.; van Gisbergen, S. J. A. *J. Phys. Chem. A* **2001**, *105*, 3311.
(25) Rosa, A.; Ricciardi, G.; Baerends, E. J. Unpublished results.
(26) Buchler, J. W.; Ng, D. K. P. In *The Porphyrin Handbook*; Kadish, K. M., Smith, K. M., Guilard, R., Eds.; Academic Press: New, York, 2000; Vol. 3, p 245.
(27) Ricciardi, G.; Rosa, A.; van Gisbergen, S. J. A.; Baerends, E. J. *J. Phys. Chem. A* **2000**, *104*, 635.

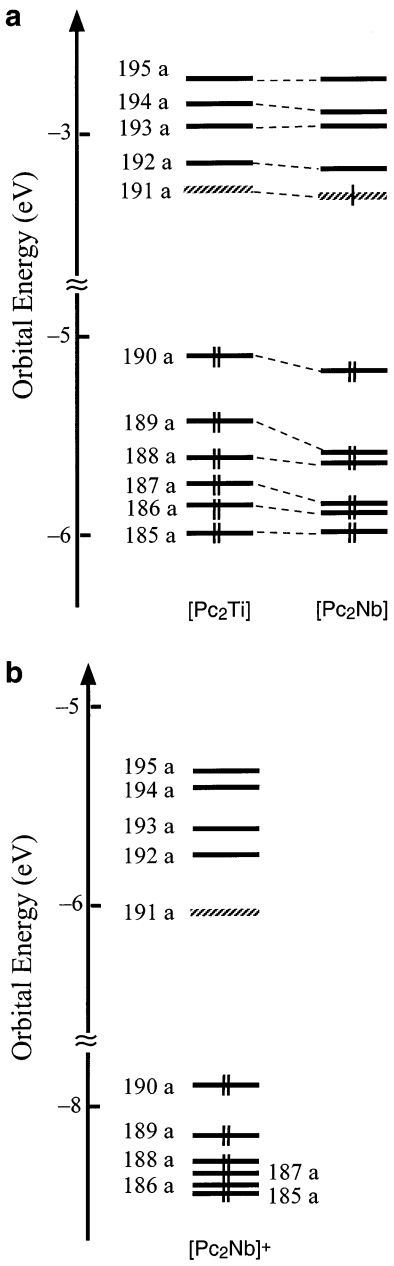

Figure 4. (a) Orbital energies for $[Pc_2Ti]$ and $[Pc_2Nb]$. For the open-shell system, $[Pc_2Nb]$, only the spin-restricted orbital energies are reported. Hatched lines indicate orbitals with prevalent metal character. (b) Orbital energies for $[Pc_2Nb]^+$. The hatched line indicates the orbital with prevalent Nb character.

4a. As for the virtual MOs, the LUMO, i.e. the 192a, is only 0.11 eV above the HOMO and is, just as the next three virtual orbitals, a macrocyclic π orbital largely localized (more than 30%) on the C_α atoms not engaged in the C−C σ bond and to a lesser extent on pyrrolic and *meso* nitrogens. The ordering and composition of the frontier orbitals of $[Pc_2Nb]$ just described are substantially the same as in its Ti(IV) analogue, $[Pc_2Ti]$, which, according to the occupation of the one-electron levels shown in Figure 4a, has a closed-shell ground-state structure. The lowest metal-centered orbital, the 191a, which in $[Pc_2Nb]$ gets occupied with one electron, is the LUMO in $[Pc_2Ti]$. The metal character of this orbital is somewhat larger than in the niobium complex (68% 3d vs 58% 4d). The self-consistent configuration of $Ti^{+1.52}$ $d^{2.48}$ $s^{0.00}$ $p^{0.00}$, again quite different from the nominal ionic state Ti^{4+} d^0 s^0 p^0, indicates that the covalent bonding interaction between the metal and the macrocycle is in titanium larger than in niobium, the $Pc_2 \rightarrow M$ donation amounting in $[Pc_2Nb]$ and in $[Pc_2Ti]$ to 1.29e and to 2.48e, respectively.

If we turn now to the electronic structure of $[Pc_2Nb]^+$, the ground state of this molecule is ^1A, with occupation of the one-electron levels as indicated in Figure 4b. Just as in $[Pc_2Ti]$, the lowest metal state is empty and is the LUMO of the molecule. Thus, the Nb atom in $[Pc_2Nb]^+$ can be formally described as Nb(V) (d^0), in keeping with the observed diamagnetism of this molecule.[6] It is worth mentioning, however, that the oxidation process induces a large charge rearrangement, consisting mainly of an increase of the $Pc_2 \rightarrow$ Nb donation. In the oxidized complex, the $Pc_2 \rightarrow$ Nb donation amounts indeed to 2.13e, a value considerably larger (about 0.8e) than in the parent neutral species. This explains why the charge of the niobium atom increases only by +0.16e going from the neutral to the oxidized complex (2.71e vs 2.87e). The shortening, by 0.03 Å, of the Nb−N_p average distance and related distances on going from $[Pc_2Nb]$ to its monocation observed experimentally (Table 3) fits in with the stronger metal−macrocycle interaction theoretically predicted for the oxidized species. DFT calculations on $[Pc_2Nb]^+$ also indicate that, apart from the generalized downward shift of the MOs induced by the positive charge on the molecule, the composition and the ordering of the frontier orbitals remain substantially the same as in the neutral molecule, as well as in the Ti(IV) analogue.

Although the marked similarities in the ground-state electronic structure of $[Pc_2Nb]$, $[Pc_2Nb]^+$, and $[Pc_2Ti]$ qualitatively account for the three complexes showing very similar UV−visible solution spectra, as inferred from those observed in CH_2Cl_2 (see Figure 3), and also in ClNP for the Ti complex (with detectable peaks at 426 and 467 nm),[1] a quantitative assessment of these similarities may only come from explicit calculations of the excited states. These calculations have been performed using TDDFT methods, whose reliability in obtaining accurate prediction of excitation energies and oscillator strengths for metallotetrapyrroles is by now well documented.[23,24,27−29] The excited-state calculations have been restricted to the two closed-shell systems, $[Pc_2Nb]^+$ and $[Pc_2Ti]$, since in the current ADF implementation of TDDFT open-shell systems such as $[Pc_2Nb]$ are not tractable. The theoretical excitation energies and oscillator strengths of the lowest allowed ^1A excited state, and of the higher (up to 3.0 eV) ^1A excited states with largest oscillator strength, are gathered in Tables 4 and 5 for $[Pc_2Ti]$ and $[Pc_2Nb]^+$, respectively, together with the experimental energy values determined from the solution spectra. According to the TDDFT results, the lowest allowed excited state is located at 1.79 eV (692 nm) and 1.97 eV (629 nm) in titanium and niobium, respectively. It corresponds to the HOMO → LUMO ligand-to-metal charge transfer transition (LMCT) and has very low oscillator strength. Up to 2.5 eV (500 nm)

(28) van Gisbergen, S. J. A.; Rosa, A.; Ricciardi, G.; Baerends, E. J. *J. Chem. Phys.* **1999**, *111*, 2505.
(29) Nguyen, K. A.; Pachter, R. *J. Chem. Phys.* **2001**, *114*, 10757.

Table 4. Calculated Excitation Energies (eV) and Oscillator Strengths for Selected Optically Allowed ^{1}A Excited States of [Pc_2Ti] Compared to the Experimental Data[a]

state	composn, %	exc energy	*f*	expt[b]
1^1A	99 (190a → 191a)	1.79	0.0006	
3^1A	93 (189a → 191a)	2.14	0.0198	
4^1A	94 (188a → 191a)	2.25	0.0234	
12^1A	87 (185a → 191a)	2.56	0.0172	2.65 (467)[c]
17^1A	44 (182a → 191a)	2.69	0.0109	
	17 (184a → 191a)			
	9 (181a → 191a)			
19^1A	61 (188a → 193a)	2.73	0.0106	
	10 (186a → 192a)			
	9 (189a → 194a)			
24^1A	17 (190a → 196a)	2.81	0.0308	2.91 (426)[c]
	17 (189a → 195a)			
	13 (178a → 191a)			
27^1A	58 (185a → 192a)	2.83	0.0185	
37^1A	24 (183a → 192a)	2.99	0.0478	
	16 (182a → 192a)			
	12 (186a → 193a)			
38^1A	39 (182a → 192a)	3.02	0.0386	
	9 (188a → 194a)			

[a] The major one-electron transitions contributing to the BP/ALDA solution vectors are also given. [b] Nanometers in parentheses. [c] Observed in the ClNP spectrum[1] and referred to also in the text.

Table 5. Calculated Excitation Energies (eV) and Oscillator Strengths for Selected Optically Allowed ^{1}A Excited States of [Pc_2Nb]$^+$ Compared to the Experimental Data[a]

state	composn, %	exc energy	f	expt[b]
1^1A	98 (190a → 191a)	1.97	0.0002	
2^1A	89 (189a → 191a)	2.20	0.0156	
13^1A	25 (183a → 191a)	2.56	0.0146	
	19 (190a → 194a)			
	11 (182a → 191a)			
26^1A	34 (186a → 192a)	2.75	0.0194	3.10−2.48
	13 (188a → 193a)			(400−500)[c]
	8 (185a → 192a)			
28^1A	38 (173a → 191a)	2.76	0.0118	
	31 (172a → 191a)			
	10 (185a → 192a)			
31^1A	37 (184a → 192a)	2.80	0.0118	
	26 (183a → 192a)			
32^1A	16 (184a → 192a)	2.82	0.0207	
	16 (183a → 192a)			
	11 (182a → 192a)			
	11 (185a → 192a)			
37^1A	30 (181a → 192a)	2.89	0.0208	
	17 (189a → 195a)			
	11 (188a → 194a)			
39^1A	17 (186a → 193a)	2.91	0.0445	
	11 (181a → 192a)			
	11 (185a → 193a)			
40^1A	25 (188a → 194a)	2.92	0.0214	
	21 (180a → 192a)			
	12 (169a → 191a)			
41^1A	31 (185a → 193a)	2.95	0.0483	
	19 (188a → 194a)			

[a] The major one-electron transitions contributing to the BP/ALDA solution vectors are also given. [b] Nanometers in parentheses. [c] CH_2Cl_2 spectrum, Figure 3, present work.

only a few excited states of appreciable intensity are computed, i.e. the 2^1A in [Pc_2Nb]$^+$ and the 3^1A and 4^1A in [Pc_2Ti]. They also have LMCT character as they involve transitions out of the highest occupied macrocycle MOs to the metal-centered LUMO orbital. What is predicted fits in with the solution spectra of the "stapled" bis(phthalocyaninato) complexes showing extremely weak absorptions on the tail just above 500 nm.

A plethora of excited states are calculated at higher energy in the region 400−500 nm. Some of them are of appreciable intensity, the latter, however, much lower than that of the Q or B phthalocyanine excited states. Most of the states are of ligand-to-ligand charge-transfer type (LLCT) and show a pronounced multitransition character. They account for the broad plateau in the 400−500 nm region, which characterizes the solution optical spectra of the "stapled" complexes and is responsible for their yellowish color.

As for [Pc_2Nb]$^+$, the broad absorption raising at ∼500 nm and extending to ∼400 nm is accounted for by the states calculated in the range 2.56−2.95 eV (484−415 nm). The calculated spectra of [Pc_2Ti] and [Pc_2Nb]$^+$ together with the ground-state electronic structures of the three sandwiched units strongly suggest that the excited states responsible for the broad absorptions in the region 400−500 nm observed in the solution spectra of all three "stapled" complexes should be located in [Pc_2Nb] approximately at the same energies as in the [Pc_2Ti] and [Pc_2Nb]$^+$ analogues. Noteworthy, the observed lowering in intensity of the plateau (400−500 nm) on going from [Pc_2Nb]$^+$ to its neutral parent (see Figure 3) is however not predictable in the absence of explicit calculations of the oscillator strengths of the involved excited states. [Pc_2Nb] will certainly feature additional metal-to-ligand charge transfer (MLCT) states involving transitions out of the singly occupied metal orbital, the 191a, into the lowest virtual orbitals. These are expected to occur however at very low energy, in the near-IR region.

Finally, as to the redox behavior of [Pc_2Nb], our calculations provide a plausible explanation for its reluctance to undergo further chemical or electrochemical (see below) oxidation. The calculated energy levels of the neutral and oxidized species clearly indicate that removal of an electron from the monocation to produce the [Pc_2Nb]$^{2+}$ species is energetically quite demanding; in fact, in [Pc_2Nb]$^+$ the 190a-HOMO, the orbital to be partially emptied, is ∼5 eV lower than the singly occupied [Pc_2Nb] 191a. Moreover, the first (vertical) ionization potential calculated for [Pc_2Nb]$^+$ is quite large (9.38 eV), much larger than the first (adiabatic) ionization potential predicted by the calculations for [Pc_2Nb] (5.78 eV).

Electrochemical and Electrochromic Studies. Examination of the electrochemical and electrochromic behavior of [Pc_2Nb] has been undertaken, since electrochromism is a widely investigated applicative target[30] and sandwich-type diphthalocyanine complexes, [Pc_2M] (M = mainly rare earth metal ions, among them particularly Lu(III)), are attractive molecular materials for their use in display devices.[31] Among the [Pc_2M] species, the "stapled" [Pc_2Ti], deposited in the form of thin films on ITO glass, was fairly recently studied[4] and cyclic voltammetric and spectroelectrochemical experiments provided evidence of UV/visible spectral and related color changes of the solid material in an anodic scan,

(30) Monk, P. S. M.; Mortimer, R. J.; Rosseinsky, D. R. *Electrochromism-Fundamentals and Applications*; VCH: Weinheim, Germany, 1995.
(31) Nicholson, M. M. Electrochromism and Display Devices. In *Phthalocyanines-Properties and Applications*"; Leznoff, C. C., Lever, A. B. P., Eds.; VCH, Inc.: Weinheim, Germany, 1993; Vol. 3, pp 71−118.

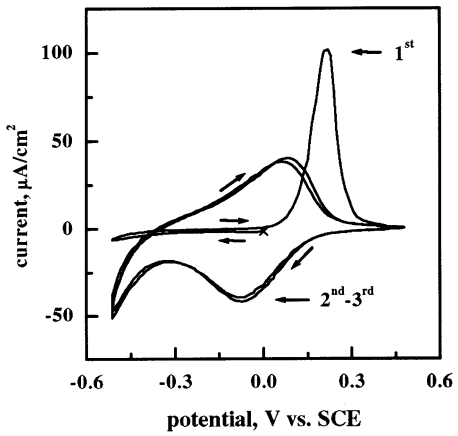

Figure 5. Cyclic voltammogram of an ITO/[Pc_2Nb] film (thickness ~ 250 nm) in contact with 1 M KCl aqueous solution (scan rate of 5 mV/s).

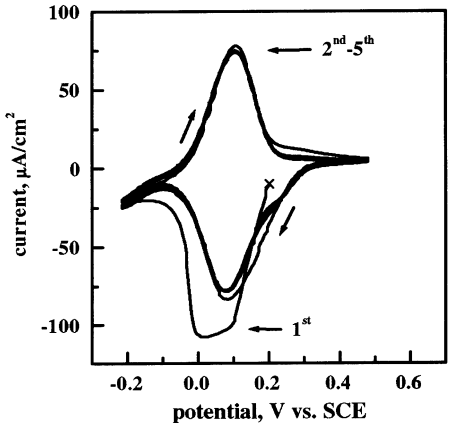

Figure 6. Cyclic voltammogram of an ITO/[Pc_2Nb] film (thickness ~ 150 nm) in contact with 1 M HCl aqueous solution (scan rate of 5 mV/s).

associated with two integral monoelectronic, forcedly ligand-centered oxidations and formation of the +1 and +2 charged fragments $[Pc_2Ti]^+$ and $[Pc_2Ti]^{2+}$. No evidence was given of, or relationship established with, the "nonintegral oxidation" occurring, instead, by chemical oxidation of [Pc_2Ti] with I_2, which leads to the formation of the electrically conducting species of formula $[Pc_2Ti](I_3)_{0.66}$.[5]

The electrochemical behavior of thin films of [Pc_2Nb] has been examined in aqueous neutral and acidic solutions. Figure 5 reports the first and the subsequent voltammetric scans in aqueous KCl solution. The first cycle displays a strong anodic peak at 210 mV vs SCE, while, upon cycling, the redox process reveals two well-defined peaks centered at −80 mV vs SCE in the cathodic scan and 10 mV vs SCE in the anodic one. The voltammetric response does not change during the subsequent cycles, indicating a fast and reversible process. A substantially similar behavior has also been observed in other neutral aqueous Cl^--based solutions (electrolytes: LiCl, NaCl, or TEACl). Noteworthy, no other redox processes are evidenced within the voltammetric range examined in the aqueous medium, nor they are in the wider anodic region explored by using a nonaqueous solvent (propylene carbonate). Since, reasonably, the observed redox process must be associated with the chemically established monoelectronic exchange between [Pc_2Nb] and its +1 corresponding fragment, it has to be concluded that no chance is given for the formation of more oxidized species, in full agreement with the above chemical observations and theoretical findings.

Penetration of Cl^- ions into the solid-state structure of the thin films for the necessary preservation of electroneutrality associated with the anodic process

$$[Pc_2Nb] + Cl^{(-)} \rightarrow [Pc_2Nb]^{(+)}(Cl)^{(-)} + e^-$$

has to be considered. In support of this, experiments clearly show that the voltammetric peak heights are proportional to the square root of the scan rates; hence, classically,[32] the electrochemical process is ion diffusion-controlled. The $Cl^{(-)}$ diffusion is assumed to have no limitation, owing to the large interspaces very likely occurring among adjacent sandwiched cationic units.

Some different behavior is observed for the electrochemical experiments conducted in strong acid aqueous solutions (1 M HCl and $HClO_4$, 0.1 M HNO_3), as might be predicted, owing to the presence of the H_3O^+ ions and of different anions. Figure 6 shows the voltammetric response of a [Pc_2Nb] electrode in 1 M HCl solution. After a fast initial reassessment, the film reaches the steady-state condition showing two well-defined peaks at 100 mV vs SCE in the anodic region and at 63 mV vs SCE in the catodic one, with a peak separation of 37 mV. Good reversibility and associated high stability of the [Pc_2Nb] system in the acidic medium are in line with observations for other known bis(phthalocyanine) molecules.[33] The different observed behavior in the acidic medium is obviously related to the high concentration of H_3O^+ ions, certainly capable of some type of interaction with the weakly basic *meso* N atoms of the phthalocyanine rings. Further information coming from the voltammetric scans in HNO_3 and $HClO_4$ (Figure 7, parts A and B, respectively), appearing very similar to one another, but well distinct from that in HCl, suggests that, indeed, the H_3O^+ ions are acting as ion pairs.

The data so far illustrated indicate that the observed redox behavior of [Pc_2Nb] is a result of different combined phenomena, among them charge transfer reactions and ion insertion and deinsertion of different nature in an aqueous medium, and the overall mechanism seems to be mass transfer limited. Some impedance measurements (frequency response analysis, FRA) have been also carried out for a better understanding of the phenomena taking place at the interface and likely to be useful in clarifying the mechanism of the whole process.[34] In this work the FRA spectra were explored over the frequency range 10 kHz−100 mHz. The overall response of a pristine [Pc_2Nb] film in KCl solution is shown in Figure 8. The impedance diagram resembles that

(32) Bard, A. J.; Faulkner, L. R. *Electrochemical Methods*; John Wiley & Sons: New York, 1980.

(33) a) Nicholson, M. M.; Pizzarello, F. A. *J. Electrochem. Soc.* **1981**, *128*, 1740. (b) Riou, M. T.; Clarisse, C. *J. Electroanal. Chem.* **1988**, *249*, 181.

(34) Macdonald J. R. In *Impedance Spectroscopy*; MacDonald, J. R., Ed.; John Wiley & Sons: New York, 1987; p 64.

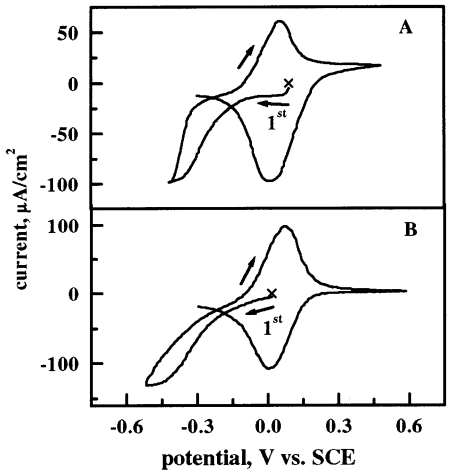

Figure 7. Cyclic voltammograms of an ITO/[Pc_2Nb] film (thickness ~ 100 nm) in contact with a 0.1 M HNO_3 aqueous solution (A; scan rate 5 mV/s) and of an ITO/[Pc_2Nb] film (thickness ~ 50 nm) in contact with a 0.1 M $HClO_4$ aqueous solution (B; scan rate 10 mV/s).

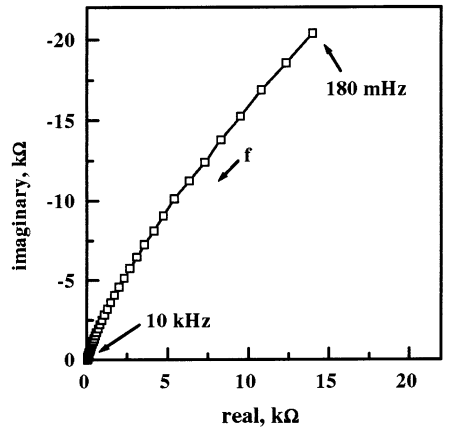

Figure 8. Impedance spectra of an ITO/[Pc_2Nb] electrode (film thickness ~ 100 nm) held at OCV = −67 mV vs SCE in contact with a 1 M KCl aqueous solution.

generally observed for a thin blocking electrode.[35] This is not unexpected, since the bis(phthalocyanine) molecule is neutral and the electrochemical response is related to a semiconductor electrode. When the [Pc_2Nb] film is polarized, the impedance spectrum (Figure 9) reveals at high frequency a semicircle that may be attributed to a charge-transfer process occurring at the electrode/electrolyte interface. The impedance response in the low-frequency range (3−0.3 Hz) displays a linear behavior with a frequency-independent phase angle of $\pi/4$. In this condition the redox process becomes controlled by the diffusion determined by the penetration of the Cl^- counterions into the [Pc_2Nb] electrode. Hence, the response is here representative of the mass-transfer parameter (Warburg impedance element).[35] With further extension of the oxidation process to high potential (≅1 V vs SCE), the impedance response resembles that of a blocking [Pc_2Nb] electrode, which prevents other redox reactions (Figure 10). Conclusively, then, no additional electrochemical processes are evidenced by the impedance measurements in this potential region, which excludes further

(35) Berthier, F.; Diard, J.-P.; Michel, R. *J. Electroanal. Chem.* **2001**, *510*, 1.

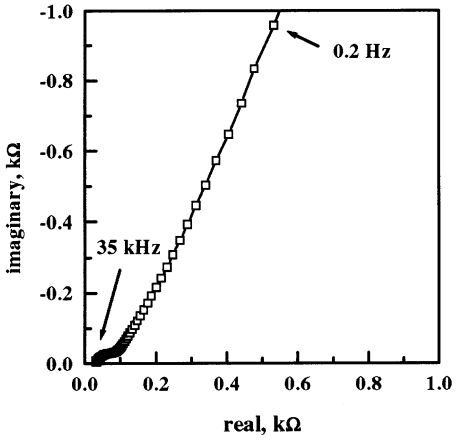

Figure 9. Impedance spectra of an ITO/[Pc_2Nb] electrode (film thickness ~ 100 nm) held at 100 mV vs SCE in contact with 1 M KCl aqueous solution.

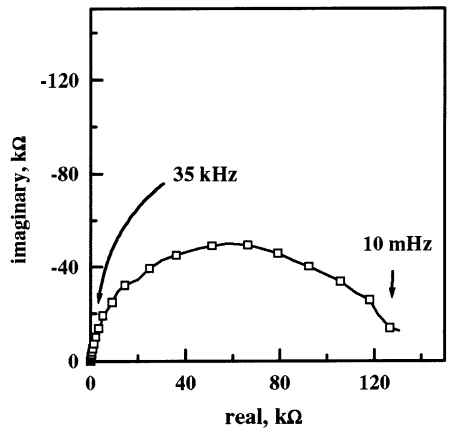

Figure 10. Impedance spectra of an ITO/[Pc_2Nb] electrode (film thickness ~ 100 nm) held at 1 V vs SCE in contact with 1 M KCl aqueous solution.

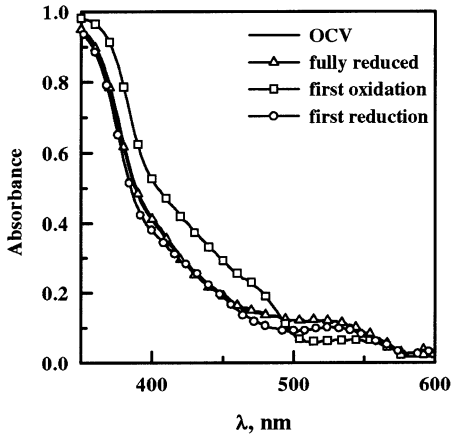

Figure 11. Electronic absorption spectral changes of an ITO/[Pc_2Nb] electrode (film thickness ~ 100 nm) during cyclic voltammetric scans in 1 M KCl aqueous media.

oxidation above the +1 charged species, in full agreement with the above chemical and theoretical findings.

[Pc_2Nb] electrodes were examined by in situ UV−visible absorption spectroscopy upon oxidation and reduction. Figures 11 and 12 show the spectral changes of [Pc_2Nb] films with applied potentials in KCl and HCl solutions, respectively. The spectra of the neutral electrodes show in the 400−500 nm region a broad very weak absorption with its tail

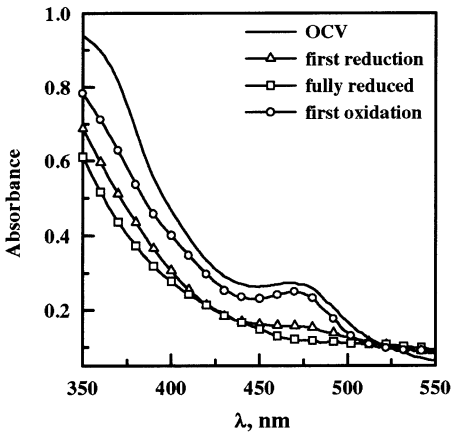

Figure 12. Electronic absorption spectral changes of an ITO/[Pc_2Nb] electrode (film thickness ~ 150 nm) during cyclic voltammetric scans in 1 M HCl aqueous media.

moving up to ca. 550 nm, undergoing in this region only subtle changes during the oxidation and reduction processes, with no changes at higher wavelengths. Noticeably, the different intensities of the spectral response of the neutral and oxidized species roughly parallel the observed behavior in CH_2Cl_2 solution. Moreover, the observed spectral variations just above 500 nm cannot justify the formation of ligand radicals in the oxidized species. This is in keeping with the observed diamagnetism of the cationic fragment $[Pc_2Nb]^+$ in the solid material and with its silent EPR spectrum[6] and is reinforced, if necessary, by its NMR spectrum which shows narrow sharp peaks typical of a diamagnetic species.

Conclusions

Elucidation of structure of bis(phthalocyaninato)niobium(IV) by X-ray work has allowed accomplishment of a quartet of otherwise so far unapproached molecular systems, their quite peculiar feature being a highly strained "stapled" structure observed for [Pc_2Ti],[1] [Pc_2Nb] (present work), and $[Pc_2Nb]^+$ in the species $[Pc_2Nb](I_3)(I_2)_{0.5}\cdot 3.5ClNP$[6] or something in close relationship with it, as in the case of $[Pc_2Ti](I_3)_{0.66}$.[3] Dissimilarly from [Pc_2Ti], [Pc_2Nb] shows exclusive tendency to undergo "integral" monoelectronic oxidation with easy formation of the +1 charged fragment, whereas it is markedly reluctant to be further oxidized. A detailed DFT investigation, rarely applied to molecular systems of such a complex structure, has led to a detailed interpretation of the ground-state electronic structure for the species examined. As to the redox properties of [Pc_2Nb], theoretical data indicate that (i) the one-electron oxidation process $[Pc_2Nb] \rightarrow [Pc_2Nb]^+$ is metal centered and involves strong charge rearrangements in the complex and (ii) the oxidation $[Pc_2Nb]^+ \rightarrow [Pc_2Nb]^{2+}$ is energetically a highly demanding process. TDDFT calculations of the excitation energies and oscillator strengths performed for the closed-shell systems, [Pc_2Ti] and $[Pc_2Nb]^+$, provide a satisfactory interpretation of their characteristic visible optical spectra and help to rationalize the similar features observed in the visible spectrum of the open-shell "stapled" complex, [Pc_2Nb].

The electrochemical redox behavior of [Pc_2Nb] films in aqueous media shows excellent cyclability in both neutral and acidic ambients, with some distinct features in the redox processes as a function of the type of the electrolytic medium. The electrochemical process is coupled with a concomitant process of insertion/deinsertion of ions from the solution to balance the charge of the films. The observed subtle UV/visible spectral changes for [Pc_2Nb] are in line with expectation, when account is taken of the parallel slight structural and electronic modifications associated with the studied redox processes. Interestingly, the use of a water medium, the reversibility of the overall redox process, and the persistent pale-yellow color feature of [Pc_2Nb] thin films are promising requisites which are stimulating further work, now in progress, for the use of the complex as an "optically passive" electrode facing an appropriate complementary partner in an all solid electrochromic device.

Acknowledgment. E.M.B. thanks the Laboratorio Dispositivi Ottici (ENEA, Casaccia. Italy) for kind hospitality. The authors wish to thank the departmental "Servizio di microanalisi" at "La Sapienza" for elemental analyses and are indebted to Dr. P. Galli for general assistance and useful suggestions during this work. Financial support from the MIUR by Grant COFIN-9903263473 is gratefully acknowledged by C.E. and A.R.

Supporting Information Available: SCHAKAL drawings, tables listing detailed crystallographic data, atomic positional parameters, and bond lengths and angles, a table containing relevant dihedral angles within the Pc units, and X-ray files in CIF format. This material is available free of charge via the Internet at http://pubs.acs.org.

IC020098D